BULLETIN OF THE POLISH ACADEMY OF SCIENCES
TECHNICAL SCIENCES, Vol. 62, No. 4, 2014
*DOI: 10.2478/bpasts-2014-0070*

Dedicated to Professor Jan Dorosz
on the occasion of his 65th birthday

# Erbium and $Al_2O_3$ nanocrystals-doped silica optical fibers

I. KASIK[1]*, O. PODRAZKY[1], J. MRAZEK[1], J. CAJZL[1], J. AUBRECHT[1], J. PROBOSTOVA[1], P. PETERKA[1], P. HONZATKO[1], and A. DHAR[2]

[1] Institute of Photonics and Electronics of the ASCR, 57 Chaberska St., 18251, Prague 8, CR
[2] Central Glass and Ceramics Research Institute, 196 Raja Mullick Rd., Kolkata, 700032, India

**Abstract.** Fibre lasers and inherently rare-earth-doped optical fibers nowadays pass through a new period of their progress aiming at high efficiency of systems and their high power. In this paper, we deal with the preparation of silica fibers doped with erbium and $Al_2O_3$ nanocrystals and the characterization of their optical properties. The fibers were prepared by the extended Modified Chemical Vapor Deposition (MCVD) method from starting chlorides or oxide nanopowders. Conventional as well as modified approaches led to a nanocrystalline mullite phase formation in the fiber cores in which erbium is dissolved. The proposed modified approach based on starting nanopowders led to improved geometry of preforms and fibers and consequently to the improvement of their background attenuation. Such nanocrystal -doped fibers can be used for ASE sources. Further improvement of fiber optical properties can be expected.

**Key words:** optical fibers, nanocrystals, Rare-earth doping, luminescence.

## 1. Introduction

Fiber lasers and amplifiers belong to one of the most spectacular achievements of photonics of the last decades. Rare-earth (RE) –doped optical fibers represent their fundamental part – the active medium. Recent progress follows admirable success of erbium-doped fibre amplifiers [1–3] – one of the key components enabling long-haul transmission and thus global penetration of the Internet. Despite the 50-year history [4] fibre lasers are nowadays passing through a new period of their dynamic progress aiming at high efficiency of systems and their high power. The latest high-power lasers for machining, cutting, welding or splicing of steel are capable to provide (Fig. 1) watts or even kilowatts of optical power [5–7].

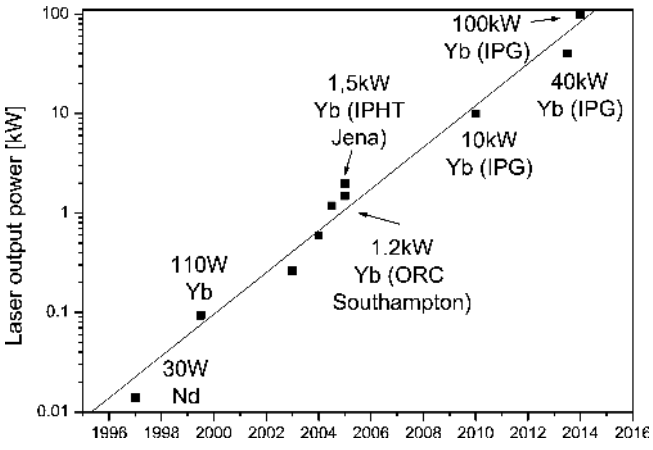


Fig. 1. Trends of the highest output powers of fiber lasers

It should be noted that the 100 kW output power was achieved by the combination of outputs of several other fiber lasers and therefore the output does not consist of only a single transversal mode. Diffraction limited, a high-quality laser beam (with the $M^2$ factor close to 1) from a single optical fiber device is nowadays limited to about 10 kW. The increase of power is believed to be possible only by the combination of more fiber laser sources [8].

Effective pumping, high conversion efficiency, high quality beam, high brightness, good thermal management, tunability, compactness and small size belong undoubtedly to the main advantages of fiber lasers. High-power laser applications are nowadays based mainly on Yb -doped fiber lasers operating at around 1060–1120 nm, Er – doped fiber lasers operating at around 1520–1550 nm and Tm – doped fiber lasers operating at around 2 microns. Erbium and ytterbium are known for high quantum conversion efficiency of almost 100%. With the pump at 980 nm it results in power conversion efficiency of about 63% for erbium- and about 93% for ytterbium-doped fiber lasers.

Special silica-based fibers are suitable for these purposes because of their low optical losses in wide transmission windows and good thermal durability. However, pure silica is not a suitable matrix for RE ions due to low solubility of RE. Their presence of only hundreds of ppm leads to phase separation. In such cases, the phase of micron-size aggregates is separated from a homogeneous glass matrix and causes a fatal increase of spectral attenuation of the fibers. Therefore, this effect must be prevented and several approaches have already been investigated up to this date.

Modification of glass matrices mainly with $Al_2O_3$, $P_2O_5$ or $Sb_2O_3$ has been practiced in silica fibers for years with the aim to increase the solubility of REs in the fiber core and so to enhance the emission [9–18].

The preparation of fibers based on soft optical glass matrices [19, 20] represents an alternative approach. RE in a large concentration span can be well dissolved in these fibers of va-

*e-mail: kasik@ufe.cz

riety of glass compositions. Higher attenuation is one of the important factors limiting their application usually feasible in a wide spectral range and lower output power.

Recent progress in nanotechnologies and sol-gel methods have brought a completely novel powerful tool to this field. When the nanoparticles of a suitable composition and size are homogeneously dispersed in a disordered matrix of any glass, the high transparency value of the material is preserved even for higher contents of RE and thus can cause an enhancement of fluorescence (Fig. 2).

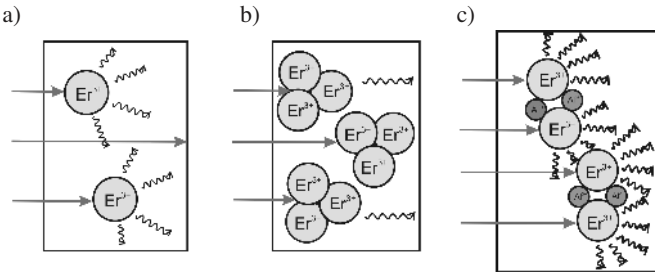


Fig. 2. A schematic image of the influence of Erclusters and nanocrystals in a disordered glass matrix on luminescence intensity: a) RE ions in low concentration distributed in a silica glass matrix produce weak luminescence, b) increased concentration of RE ions results in the formation of clusters decreasing the luminescence, c) the effect of nanoparticles results in higher concentration of RE ions well distributed in the glass matrix and improving the luminescence properties of the material

RE – doped fibers have been modified with nanoparticles of noble metals [21, 22], semiconductors [23], ceramics like $Al_2O_3$, $TiO_2$, $ZrO_2$ and RE-containing nanocrystals [24]. Several concepts of the preparation like direct nanoparticle deposition [25], phase nano-separation [26] or the extended solution doping method [27] have been elaborated.

In this paper, we deal with the preparation of silica fibers doped with erbium and $Al_2O_3$ nanocrystals and the characterization of their optical properties.

## 2. Experimental part

Preforms suitable for fiber drawing with their cores doped with erbium and $Al_2O_3$ were prepared by the Modified Chemical Vapor Deposition method (MCVD) combined with the solution doping technique. Thin porous layers deposited from $SiCl_4$ (Merck, FO Optipur) with the flow rate of 400 ml/min at a temperature reduced to 1550°C were soaked with an ethanolic solution of chlorides or with dispersion of nanopowders of oxides in ethanol. Starting materials – $AlCl_3$ (99.99, powder Aldrich) and $ErCl_3$ (99.997, powder Aldrich) – were used in the conventional way of preparation by solution-doping [9]. Nanopowders of $Al_2O_3$ (size $<$50 nm, Sigma-Aldrich) and $Er_2O_3$ (size 41–53 nm, MaTeck GmbH) were used in the modified solution-doping approach [27]. After careful drying the layers were sintered at pure oxygen atmosphere at temperature gradually increasing from 1100°C to 1900°C. Deposited tubes were slowly collapsed at around 2200°C in oxygen atmosphere. Fibers of diameter of 125 $\mu$m were drawn at 1970°C and coated with conventional UV-curable acrylate DeSolite 3471-3-14.

Reference bulk samples for X-ray diffraction analysis (XRD) were prepared by mixing the employed precursors together with silica soot (size $<$20 nm, Sigma-Aldrich). The molar ratio of $Al_2O_3$ over $Er_2O_3$ was the same as in the preforms, however, the concentration of silica was lowered to 80 mol%. The powders were homogenized and thermally processed just in the same way as the preforms.

Concentration profiles of preforms were determined by Electron Probe Microanalysis – EPMA (Cameca SX-100). Phase contrast of preforms was characterized by secondary and back-scattered electrons (EPMA) and by optical microscopy. Preforms for fiber drawing were characterized by refractive index profile using A2600 profiler (Photon Kinetics). Data obtained with radial resolution 5 $\mu$m were recalculated to a profile of optical fiber of diameter 125 $\mu$m. XRD of reference bulk samples was performed on a Philips X'Pert PW3020 diffractometer with Bragg-Brentano geometry using a secondary graphite monochromator, a point proportional detector, and Co-K$\alpha$ radiation ($\lambda = 1.788970$ Å, operating voltage 10 kV, current 10 mA, integration time 3 s).

Spectral attenuation of the drawn fibers was determined by the cut-back method using a halogen lamp and an optical spectrum analyzer AQ-6315 (Ando). Short segments of fibers of around 0.5 m were used for the characterization of absorption bands between 600 nm and 1100 nm. Long fibers from tens to hundreds of meters in length were used for the characterization of background attenuation at 700, 1100 or 1310 nm. The background attenuation of fibers was checked using an Optical time domain reflectometer (OTDR) Exfo FTB-720-023B-04B-XX. Pulses of duration of 5 ns at 1310 nm were applied.

Fluorescence spectra of fibers were characterized using a laser diode (LD) EM4 PowerNetix operating at 976.6 nm and an optical spectrum analyzer AQ-6315 (Ando). Fluorescence lifetimes of the $^4I_{13/2}$ energy levels (metastable level) of the erbium-doped fibers were measured using the measurement setup depicted in Fig. 3. A generator (Agilent 3351 2B), a power source ILX LCM-39437, a detector (Thorlabs PDA10D-EC), an osciloscope (Agilent DSO3102A) and the same LD EM4 were used in these measurements. Short length of erbium-doped fiber and low excitation power was used to minimize the effect of amplified sponatenous emission to the fluorescence lifetime measurement.

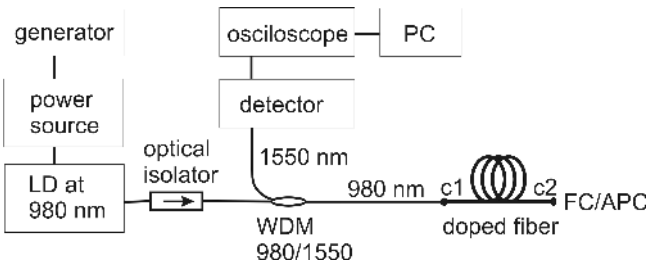


Fig. 3. Lifetime measurement scheme

Optical gain was determined by the implementation of the doped fibers into the circuit depicted in Fig. 4.

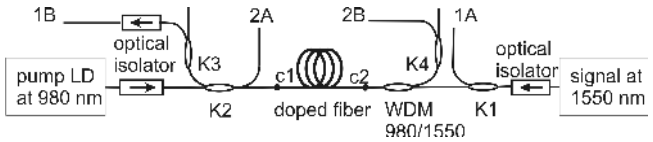


Fig. 4. Scheme of optical gain measurement. (K1, K2, K3 K4 – coupler, WDM – Wavelength-Division Multiplexer, 1A – signal input monitor, 2A – pump input monitor, 1B – signal output monitor, 2B – pump output monitor)

The net fiber gain was calculated (Eq. (1)) as:

$$gain[\mathrm{dB}] = 10\log(C1/C2) = 10\log\left([1\mathrm{B} * K3 * K2/E]/[1\mathrm{A} * K1 * E/WDM]\right), \quad (1)$$

where $E$ as an experimental constant ($E = 0.92$) and coupler ratios ($K1 = 45$, $K2 = 2.1$, $K3 = 45.1$, $WDM = 3.5$) were measured and the mean values were taken for calculation.

The setup for the measurement of backward amplified spontaneous emission (ASE) of fibers is depicted in Fig. 5.

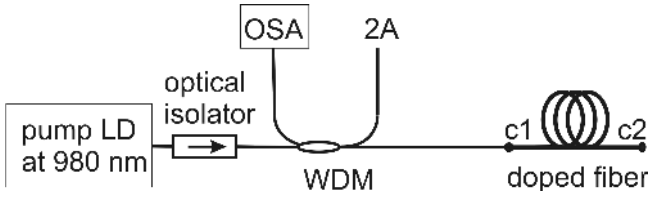


Fig. 5. Scheme of amplified spontaneous emission measurement (OSA – optical spectrum analyzer, WDM – Wavelength-Division Multiplexer, c1, c2 – beginning and end of doped fiber)

The tested fiber was cut-back and it was necessary to roughen its end to eliminate backward reflections. The output optical power was measured by OSA Ando AQ 6315 within 1520 nm and 1620 nm with its resolution of 10 nm when pumped by 144 mW of the laser diode.

## 3. Results and discussion

The used preform and fiber denoted with NANO (nanocrystal containing – SG1066) were prepared using starting nanopowders. To be able to characterize their properties and effects of nanocrystals a reference preform and a CON (conventional – SG1092) fiber were prepared by the conventional way for comparison.

The concentration profiles (Fig. 6) of the prepared preforms were nearly identical exhibiting no central dip around the axis, maximum $Al_2O_3$ content of about 5 mol% and high average erbium content of about 0.24 mol% (2400 ppm). No $GeO_2$ or $P_2O_5$ was present.

Optical transmission microscopy images of preform cores can be seen in Fig. 7a and 7b. The quite rough structure of the CON preform with beam-like imperfections on the core-cladding boundary and the smooth structure of the NANO preform were observed. An image of a totally phase separated preform core due to high RE content was taken for comparison (Fig. 7c).

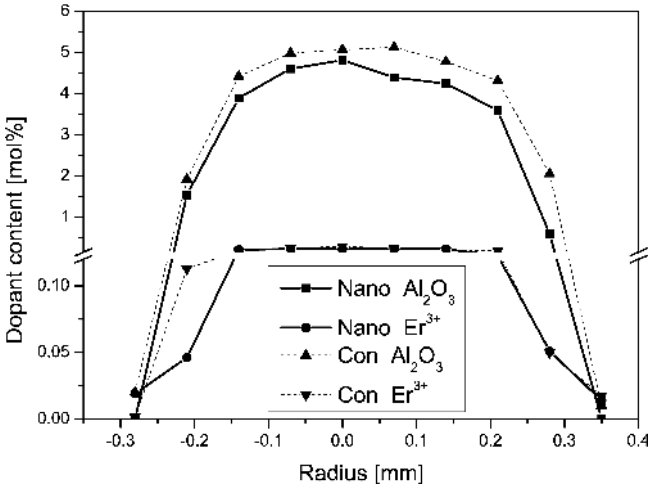


Fig. 6. Concentration profile of preforms for fiber drawing

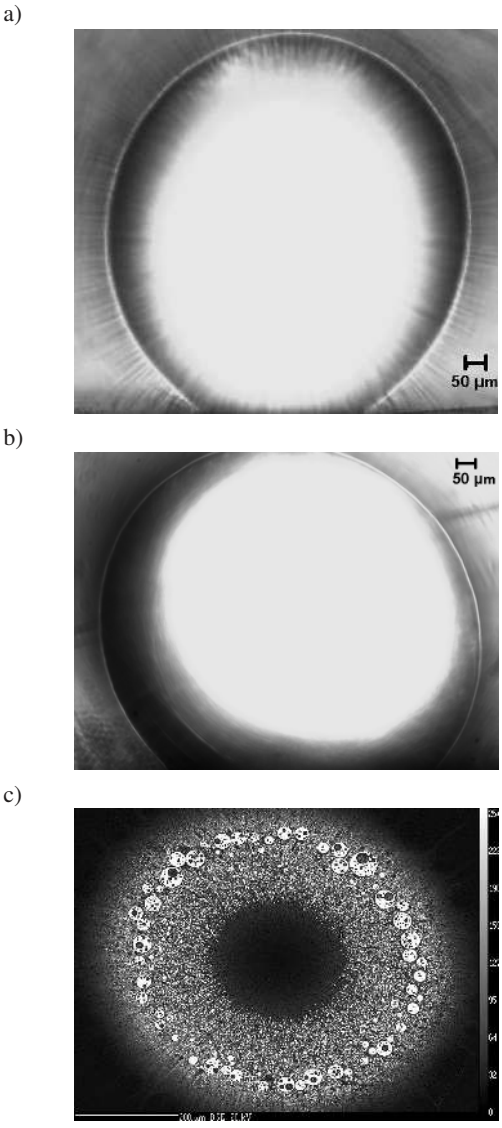


Fig. 7. Images of preform core: a) CON preform (optical microscopy); b) NANO preform (optical microscopy); c) image of a typical phase with separated core taken by secondary electrons (EPMA)

The cores of the prepared fibers represented only less than 1% of mass of the samples (see Fig. 8) and so the XRD of all the fiber samples was not sufficiently sensitive. Since it was extremely difficult to extract individual cores from fibers for the analysis, bulk reference samples were prepared. $SiO_2$ content in the reference samples was decreased in order to allow XRD above its detection limit. Typical XRD record of a reference sample can be seen in Fig. 8.

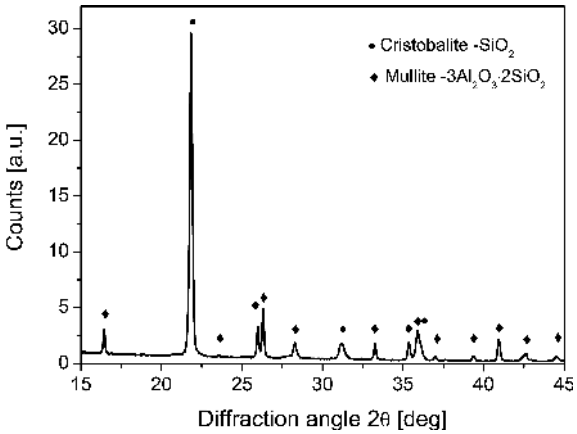


Fig. 8. XRD analysis of the reference sample prepared from starting nanopowders (NANO) and silica soot

Two phases were identified in both reference samples. The alumina precursors reacted with the silica soots forming the mullite phase ($3Al_2O_3$. $2SiO_2$). The surplus of the silica led to the formation of the cristoballite phase. Any side formation of the crystalline erbium dioxide was not observed in the XRD records. The mullite phase originates from high-temperature processing of samples at above 2100°C (i.e. above liquidus of $SiO_2$, $Al_2O_3$ or mullite) corresponding to a collapse of preforms or fiber drawing. This crystalline phase was invisible within the micron-resolution of optical microscopy, however its existence was proved by the XRD.

Refractive index profiles of fibers drawn from prefoms can be seen in Fig. 9. Profiles were recalculated from data obtained by the characterization of preforms. Both fibers were of nearly identical numerical aperture of around 0.18 and core diameter of 6 $\mu$m.

Spectral attenuation of fibers can be seen in Fig. 10. Nearly identical absorption bands caused by erbium were observed in both cases. It is in good agreement with the results obtained by EPMA and confirms a nearly identical erbium content in the samples.

Minimum background attenuation of the CON fiber at 700 nm was of about 0.74 dB/m and a much lower value of about 0.04 dB/m measured at 1100 nm was reached with the NANO fiber. Measurements of spectral attenuation were checked by OTDR at 1310 nm and good agreement was reached. All these results are in good agreement with the character of cores depicted in Fig. 7a and 7b. Improvement of background attenuation due to nanoparticle doping can be concluded from these results. Incorporation of alumina and erbium in the silica matrix become more uniform due to the relatively smaller size of the used nano-powder during the sintering of soaked soot layer in case of the NANO sample.

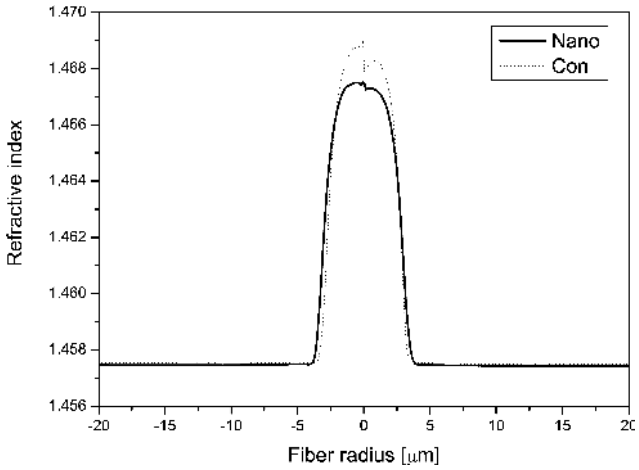


Fig. 9. Refractive index of NANO and CON fibers

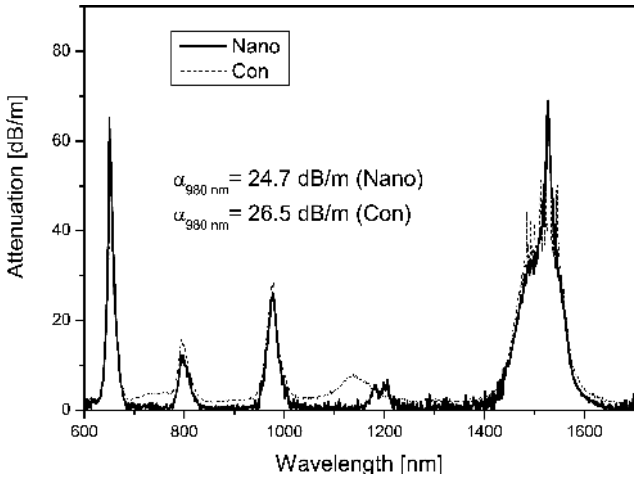


Fig. 10. Spectral attenuation of NANO and CON fibers

Normalized fluorescence spectra of the fiber samples can be seen in Fig. 11. Nearly identical fluorescence spectra were observed.

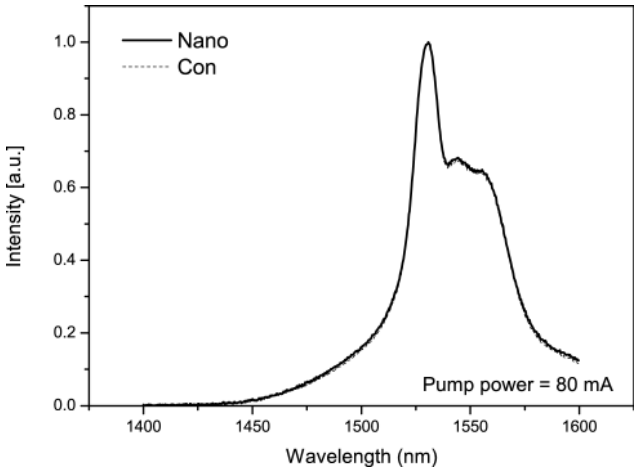


Fig. 11. Fluorescence spectra of NANO and CON fibers excited at 980 nm

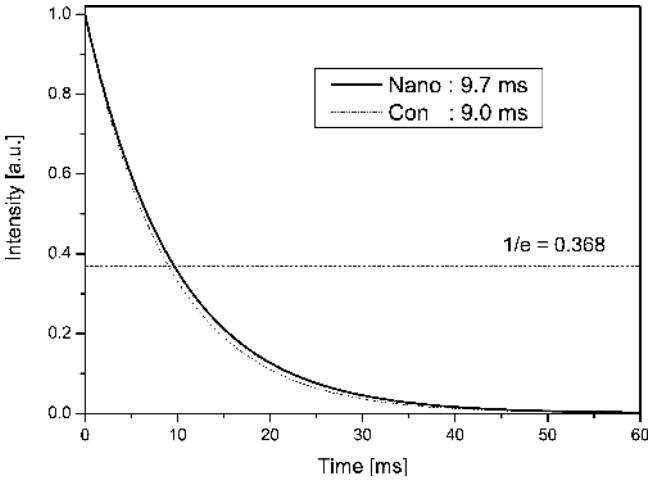


Fig. 12. Measurement of the lifetime of NANO and CON fibers

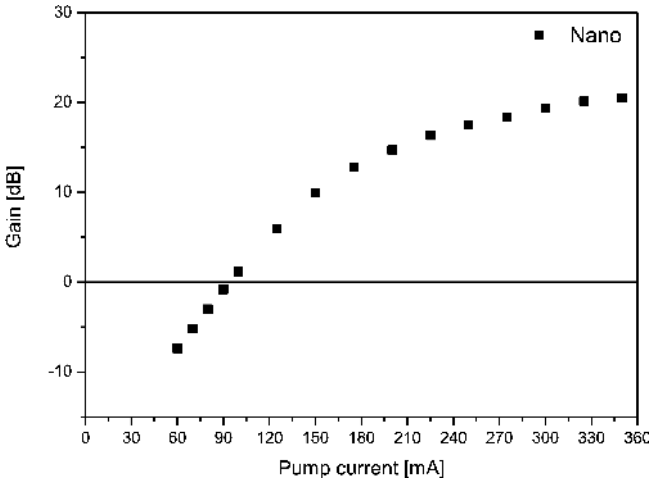


Fig. 13. Measurement of optical gain of the NANO fiber of non-optimized length

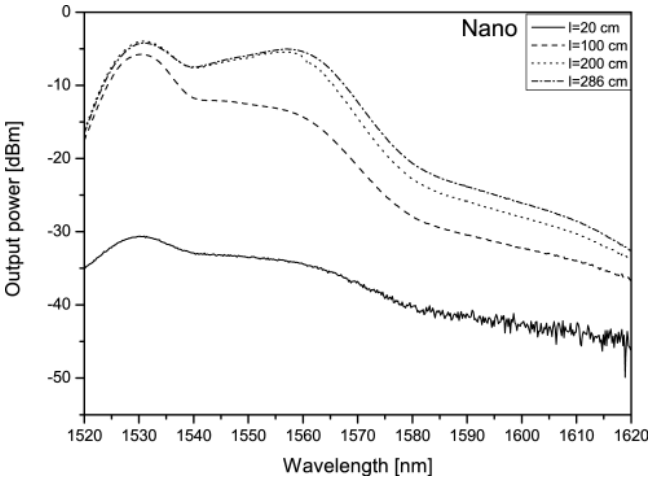


Fig. 14. Backward ASE of the NANO fiber

Using a time-resolved spectroscopy (Fig. 12) lifetime of erbium fluorescence was determined to be 9.0 ms in case of the CON fiber and 9.7 ms for the NANO fiber. The extension of erbium lifetime in fiber NANO is not so substantial, nevertheless, it supports the thesis of existence of nanocrystals inside the fiber core which follows from the XRD spectra.

Optical gain (Fig. 13) was observed from fiber NANO of non-optimized length implemented into a backward gain set-up (Fig. 4). The gain up to 20 dB was obtained when the pump threshold was 25.4 mW.

Backward ASE of fiber NANO (Fig. 14) was characterized using the setup depicted in Fig. 5.

Such fibers can be used for ASE source operating in 1520–1570 nm wavelength.

## 4. Conclusions

Optical fibers doped with nanocrystals were prepared by conventional solution doping from starting chlorides and by the modified approach from oxide nanopowders. The proposed modified approach based on starting nanopowders led to improved geometry of the preforms and fibers and so to the overall improvement of their background attenuation. Luminescence properties of both fibers were comparable. Both the conventional as well as the modified approach led to the nanocrystalline mullite phase formation in the fiber cores in which erbium is dissolved. This principle can be expected for the doping of silica fibers with alumina and any RE. Employment of reference bulk samples turned out to be an effective tool for material study in this field.

The prepared fibers doped with nanocrystals can be used for EDFA and broadband ASE sources at around 1550 nm. Further improvement of fiber optical properties can be expected on the basis of the results achieved particularly when other kinds of starting nanoparticles would be used.

**Acknowledgements.** This work was financially supported by the project M100671202 of the Grant Agency of Academy of Sciences.

REFERENCES

[1] S.B. Poole, D.N. Payne, R.J. Mears, M.E. Fermann, and R.I. Laming, "Fabrication and characterization of low-loss optical fibers containing rare-earth ions", *J. Lightwave Technology* LT-4 (7), 870–876 (1986).

[2] E. Desurvier, J.R. Simpson, and P.C. Becker, "High-gain erbium-doped travelling-wave fiber amplifier", *Optics Letters* 12 (11), 888–890 (1987)

[3] M.J.F. Digonnet, *Rare-Earth Doped Fiber Lasers and Amplifiers*, Marcel Dekker, New York, 2001.

[4] C.J. Koester and E. Snitzer, "Amplification in a fiber laser", *Applied Optics* 3 (10), 1182–1186 (1964).

[5] Y. Jeong, J.K. Sahu, D.N. Payne, and J. Nilsson, "Ytterbium-doped large-core fibre laser with 1.36 kW continuous-wave output power", *Optics Express* 12 (25), 6088–6092 (2004).

[6] D.N. Payne, Y. Jeong, J. Nilsson, J.K. Sahu, D.B. S. Soh, C. Algeria, P. Dupriez, C.A. Codemard, V.N. Philippov, and V. Hernandez, "Kilowatt-class single-frequency fiber sources", *Proc. SPIE* 5709, 133–141 (2005).

[7] V.P. Gapontsev, "Advances and opportunities in fiber lasers" *SPIE Photonics* 1, CD-ROM (2013).

[8] P. Honzatko, Y. Baravets, F. Todorov, P. Peterka, and M. Becker, "Coherently combined 20 W at 2000 nm from a pair of thulium-doped fiber lasers", *Laser Phys. Lett.* 10 (9), 095104–095105 (2013).

[9] J.E. Townsend, S.B. Poole, and D.N. Payne, "Solution-doping technique for fabrication of rare-earth-doped optical fibres", *Electronics Letters* 23 (7), 329–331 (1987).

[10] B.J. Ainslie, S.P. Craig, S.T. Davey, and B. Wakefield, "The fabrication, assessment and optical properties of high-concentration $Nd^{3+}$ and $Er^{3+}$ – doped silica-based fibers", *Materials Letters* 6 (5–6), 139–144 (1988).

[11] O. Sysala, I. Kasik, and I. Spejtkova, "Preparation of preforms and optical fibres containing aluminum by the solution-doping method", *Ceramics-Silikaty* 35 (4), 363–367 (1991).

[12] A.L.G. Carter, S.B. Poole, and M.G. Sceats, "Flash-condensation technique for the fabrication of high-phosphorus-content rare-earth-doped fibers", *Electronics Letters* 28 (21), 2009–2011 (1992).

[13] G.G. Vienne, J.E. Caplen, L. Dong, J. D. Minelly, J. Nilsson, and D.N. Payne, "Fabrication and characterization of $Yb^{3+}$: $Er^{3+}$ phosphosilicate fibers for lasers", *J. Lightwave Technology* 16 (11), 1990–2000 (1998).

[14] D. DiGiovanni, R. Shubochkin, T.F. Morse, and B. Lenardic, "Rare earth – doped fibers", in *Specialty Optical Fibers Handbook*, ed. A. Mendez, T.F. Morse, Chapt. 7, Elsevier, Amsterdam, 2007.

[15] M.M. Bubnov, V.N. Vechkanov, A.N. Gur'yanov, K.V. Zotov, D.S. Lipatov, M.E. Likhachev, and M.V. Yashkov, "Fabrication and optical properties of fibers with an $Al_2O_3$-$P_2O_5$-$SiO_2$ glass core", *Inorganic Materials* 45 (4), 444–449 (2009).

[16] J. Kirchhof, S. Unger, A. Schwuchow, S. Jetschke, V.Reichel, M. Leich, and A. Scheffel, "The influence of Yb2+ ions on optical properties and power stability of ytterbium doped laser fibers", *Proc. SPIE* 7598, 75980B (2010).

[17] A. Dhar, S. Das, and H.S. Maiti, "Fabrication of high aluminium containing rare-earth doped fiber without core-clad interface defects", *Optics Communications* 283 (11), 2344–2349 (2010).

[18] B. Dussardier, J. Maria, and P. Peterka, "Passively Q-switched ytterbium- and chromium-doped all-fibre laser", *Applied Optics* 50 (25), E20–E23 (2011).

[19] D. Dorosz, J. Zmojda, and M. Kochanowicz, "Investigation on broadband near-infrared emission in $Yb^{3+}$/$Ho^{3+}$ co-doped antimony-silicate glass and optical fiber", *Optical Materials* 35 (12), 2577–2580 (2013).

[20] J. Zmojda, D. Dorosz, and J. Dorosz, "2.1 $\mu$m emission of $Tm^{3+}$/$Ho^{3+}$ – doped antimony-silicate glasses for active optical fibre", *Bull. Pol. Ac.: Tech.* 59 (4), 381–387 (2011).

[21] A. Lin, S. Boo, S. Moon, H. Jeong, Y. Chung, and W.T. Han, "Luminescence enhancement by Au nanoparticles in $Er^{3+}$ – doped germano-silicate optical fibre", *Optics Express* 15 (14), 8603–8608 (2007).

[22] P.R. Watekar, S. Ju, and W.T. Han, "Optical properties of the alumino-silicate glass doped with Er-ions/Au particles", *Colloids and Surfaces: Physicochemical and Engeneering Aspects. Special Issue* A 313, 492–496 (2008).

[23] S. Moon, A. Lin, B.H. Kim, P.R. Watekar, and W.T. Han, "Linear and nonlinear optical properties of the optical fibre doped with silicon nano-particles", *J. Non-Crystalline Solids* 354 (2–9), 602–606 (2008).

[24] J. Mrazek, L. Spanhel, G. Chadeyron, and V. Matejec, "Evolution and $Eu^{3+}$ doping of Sol-gel derived ternary $Zn_xTi_yO_z$ – nanocrystals", *J. Physical Chemistry* C 114, 2843–2852 (2010).

[25] J. Koponen, L. Petit, T. Kokki, V. Aallos, J. Paul, and H. Ihalainen, "Progress in direct nanoparticle deposition for the development of the next generation fibre lasers", *Optical Engineering* 50 (11), 111605 (2011).

[26] A. Dhar, I. Kasik, B. Dussardier, O. Podrazky, and V. Matejec, "Preparation and properties of Er–doped ZrO2 nanocrystalline phase-separated preforms of optical fibres by MCVD process", *Int. J. Applied Ceramic Technology* 9, 341–348 (2012).

[27] O. Podrazky, I. Kasik, M. Pospisilova, and V. Matejec, "Use of nanoparticles for preparation of rare-earth doped silica fibers", *Physica Status Solidi – Current Topics In Solid State Physics* C 6, 2228–2230 (2009).